



Geochemical modeling and isotopic approach for delineating water resources evolution in El Fayoum depression, Egypt

E. Srour¹ · R. A. Hussien¹ · W. M. Moustafa¹

Received: 7 August 2020 / Accepted: 4 January 2022 / Published online: 5 February 2022
© The Author(s) 2022

Abstract

In this study, an attempt was made to understand the hydrogeochemical processes controlling water resources (surface and groundwater) evolution in El Fayoum depression, Egypt. Hydrochemical, inverse geochemical modeling integrated with environmental isotopes was applied. Forty-three surface and groundwater samples were collected and analyzed for major chemistry (cations, anions) and environmental stable isotopes ($\delta^{18}\text{O}$, δD). The ionic sequence based on relative molar proportions for cations was $\text{Na}^+ > \text{Ca}^{2+} > \text{Mg}^{2+} > \text{K}^+$ and $\text{Na}^+ > \text{Mg}^{2+} > \text{Ca}^{2+} > \text{K}^+$ for surface and groundwater, respectively and for anions was $\text{HCO}_3^- > \text{Cl}^- > \text{SO}_4^{2-}$ for all water samples. $\delta^{18}\text{O}$ and δD relationship plot on a typical evaporation line, enhance potential evaporation of recharging water prior to infiltration. Saturation index estimation revealed that water resources were affected by carbonate and evaporites minerals dissolution and supersaturated with Goethite, Gibbsite and Barite minerals. Inverse geochemical modeling using PHREEQC was used to identify water resources evolution in the study area through two flow paths A, B. The inverse model was constrained so the primary mineral phase including calcite, Aragonite, Anhydrite and Gypsum with Carbon dioxide (gas) are constrained to dissolve until they reach saturation, Whereas $\text{H}_{2(\text{g})}$, hydrogen sulphide (gas) and $\text{O}_{2(\text{g})}$ are constrained to out gas in all models for flow path (A). For flow path (B), Dolomite, Anhydrite and Gypsum are tend to dissolve with carbon dioxide (gas), $\text{H}_{2(\text{g})}$ and $\text{O}_{2(\text{g})}$ gases tend to outgassed. Finally, two processes controlling water resource evolution; carbonate and evaporites dissolution and development of cation exchange process through the aquifer system.

Keywords Hydrogeochemical processes · Environmental stable isotopes · Geochemical modeling · El Fayoum depression · Egypt

Introduction

El Fayoum area is one of most important agricultural lands of Egypt for a long time due to good soil cover and high crop productivity, In addition to it has a beauty nature represented by natural springs, waterfalls and the great natural lake (Qaroun Lake). El Fayoum's water enters through two main gated intakes, one being the natural channel Bahr Youssef, the other Bahr Hassan Wasef a canal dug in 1905 (Wolters et al. 1987). There are two main drains; The Bats in the east and the Wadi in the west. All drainage water discharged into Qaroun Lake. Population growth and increase of human activities cause several problems in El Fayoum area such as water logging and

soil salinization; these problems have already emerged after High Dam construction. Mismanagement of agricultural fertilizers and pesticides, reuse of drainage water for irrigation, wastewater disposal and inadequate land use planning had a major impact on groundwater degradation and soil quality in the studied area. Qaroun Lake, a closed saline lake acts as a natural discharging system for agricultural drainage water in El Fayoum depression. Previous studies focused mainly on this lake (Mansour and Sidky 2002, 2003; Gupta and Abd El-Hamid 2003) to investigate the influence of those waters on the lake water quality. As the groundwater resource in El Fayoum depression is a Quaternary aquifer that shows increasing signs of quality deterioration (Abdel Kawy and Belal 2012; Gad and El-Zeiny 2016; Gad and Hattab 2019) attributed to irrigation return and anthropogenic activities. The quality of water is a function of its physiochemical parameters that reflect groundwater characteristics and factors that controlling the quality of water (Hussein et al. 2017; Mgbenu and Egbueri

✉ R. A. Hussien
Rashahussien76@yahoo.com

¹ Egyptian Nuclear and Radiological Regulatory Authority, Cairo, Egypt

2019). Chemical composition of groundwater is controlled by many factors include composition of precipitation, geological structure, mineralogy of aquifers, and geochemical processes within the aquifer. The interaction of all factors leads to various water facies. Usually, major ion studies are used to define hydrochemical facies of waters and the spatial variability that can provide insight into aquifer heterogeneity and connectivity (Murray, 1996; Rosen and Jones 1998). A number of geochemical models have been developed to investigate geochemical reactions occurring along flow paths within groundwater systems. Geochemical modeling of aqueous systems is based on the assumption of chemical equilibrium among the dissolved species (Plummer 1992). Hydrogeochemical processes including dissolution, precipitation, ion-exchange, sorption and desorption together with the residence time occurring along the flow path, control the variation in chemical composition of groundwater (Apodaca et al. 2002), that can be modeled by inverse geochemical models. Inverse geochemical modeling attempts to account for the chemical changes that occur as water evolves along a flow path. Assuming two water analyses, that represent starting and final water composition along the flow path within a groundwater system, inverse modeling is used to calculate the moles of minerals and gases that must enter or leave solution to account for the differences in composition. The use of geochemical models is increasing in addressing groundwater quality problems involving geochemistry (Slimani et al. 2015; Berihu et al. 2017; Liu et al. 2020). Environmental stable isotopes (δO^{18} , δD) modified by meteoric processes provide relevant and useful tracers to identify flow regimes and sources of groundwater recharge (Leontiadis et al. 1988). Frequently, groundwater retains its stable isotopic signatures unless diluted or mixed with waters of different isotopic compositions (Fontes 1980; Gat 1981). Therefore, water from different sources or those exposed to different processes such as evaporation and / or mixing often acquire identifiable isotopic composition which can serve as natural tracers. In this paper, physical, hydrogeochemical information integrated with isotopic data were incorporated into the inverse geochemical modeling to delineate water evolution in El Fayoum depression. Hence, the objectives of this study were: (1) identify various factors affecting water (surface and groundwater) hydrogeochemical processes to understand and distinguish between the water–rock interaction and anthropogenic influences (2) characterize and assess recharge areas and the origin of surface and groundwater in the study area (3) Understand the geochemical evolution of water resources as an essential part in water management and remediation processes with a better knowledge of how the groundwater system functions.

Geology and hydrogeology

El Fayoum area is a green, fertile, near-circular depression and it has a unique physical and environmental setting. El Fayoum area occupies one of the spectacular depressions in Western Desert of Egypt, about 90 km southwest of Cairo between latitudes $29^{\circ} 00'$ and $29^{\circ} 40'$ N and longitudes $30^{\circ} 20'$ and $31^{\circ} 05'$ E (Fig. 1b). It is surrounded by desert terrain except for the southeastern side, where it is connected to the Nile Valley by the Bahr Youssef canal which derives its water from Al Ibrahimya Canal. The depression is limited at the north-western side by a shallow brackish lake, called Birket Qarun (or Lake Qarun), with an area of about 200 km² and forming the deepest part at about 45 m below the mean sea level (msl). The total surface area of El Fayoum depression is approximately 6000 km². About 1800 km² of the depression is filled with rich alluvial sediments and more than 1580 km² is cultivated. This area represents more than 5% of the total cultivated area of Egypt. It is an area of intensive agriculture, reliant solely on irrigation from the Nile River. El Fayoum depression has a special irrigation system due to the nature of its land which slopes downward from south to north. The wastewater flows from south to north towards the slope where it pours into Qarun and Wadi Al Rayan Lakes, the main sources of water drainage for the agricultural lands in the depression (UNDP 2003). Population of El Fayoum is about 2 million and the density of population is about 1000 people per km². The overall climate of this area is characterized by hot, long and dry summers and warm, short winters with scarce precipitation. Also, great temperature differences between summer and winter and between day and night characterize this belt. The temperature ranges between 46.7 and 35.1 °C in summer months and from 20 to 21.5 °C during winter months. The average annual rainfall is around 10.3 mm which is relatively low. The total annual evaporation intensity reaches 2296 mm/year, and the annual mean of relative humidity is 51.6%.

El Fayoum basin was formed initially during the Jurassic Period, probably by wind erosion in the desert, and its current shape created from tectonic subsidence that terminated in the late Eocene Epoch. The basin then subsided relative to the Nile, allowing the river to break through in flood and deposit fertile alluvial sediments. Rock units that exposed in El-Fayoum region range from Eocene to Quaternary Ages as shown in Fig. 2c. In the study area, the subsurface stratigraphic column is capped by the Pleistocene deposits that are widely distributed over the entire area of El Fayoum area. These deposits are mainly of fluvio-lacustrine origin. The Quaternary lacustrine deposits dominate in the south of Qaroun Lake, which consist of clay stone, gypsum and calcareous materials intercalated with ferruginous sandy silt (Redwan and Elhaddad 2017). The Quaternary sediments

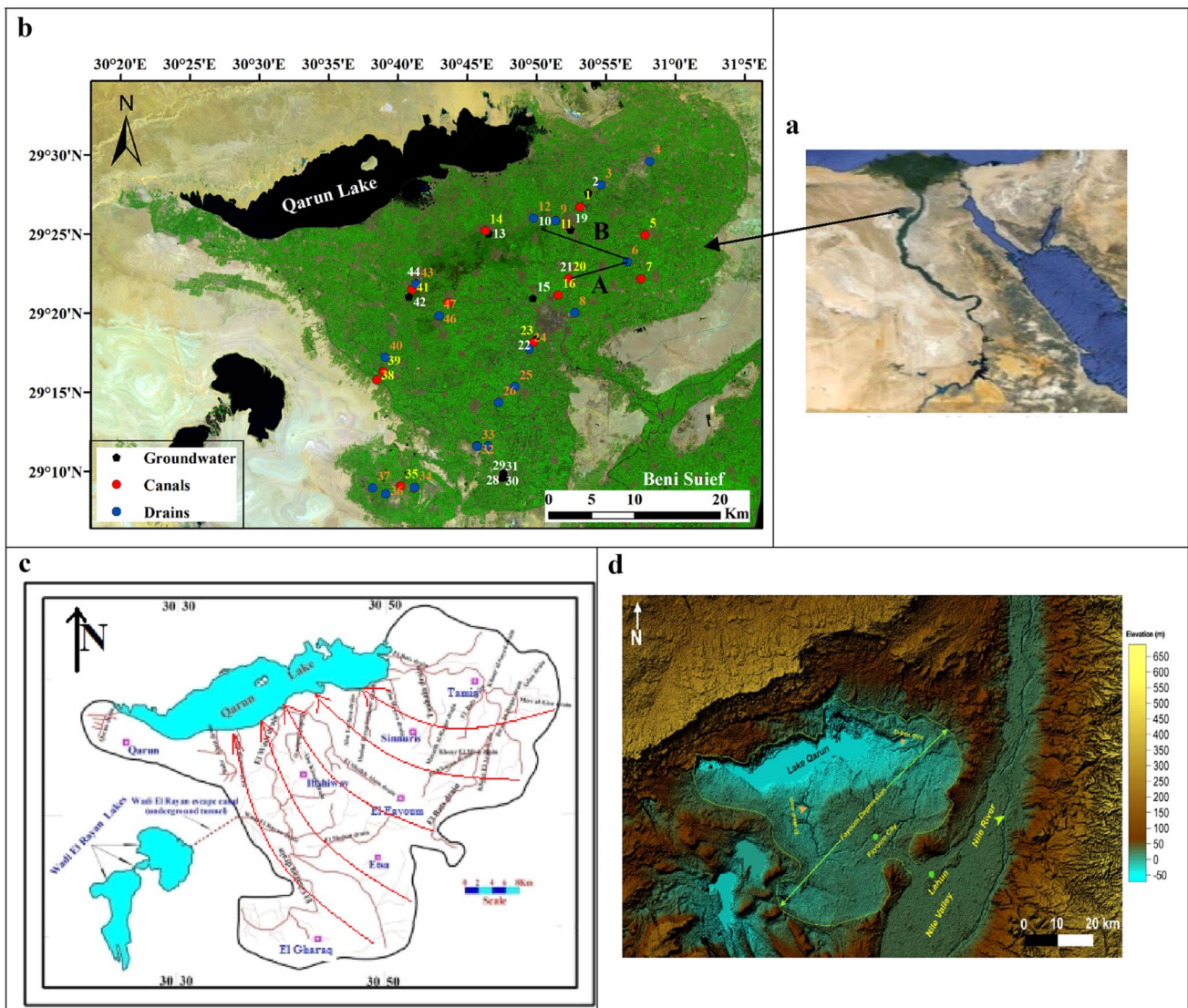


Fig. 1 a Map of the study area; b water samples location and geochemical modeled flow lines in the study area; c drainage network in El Fayoum depression with a groundwater flow direction; d digital elevation model (DEM)

overlay the Middle Eocene deposits, which are composed of limestone, marl, sand, and gypsiferous shale that outcrop around the depression (Metwaly et al. 2010). The Middle Eocene deposits overlay the Oligocene deposits, which are composed of fluvio-marine variegated sands and sandstone, with alternating shale, marls, and calcareous beds. The Lower Miocene sediments are composed of continental sandstones and conglomerates, while sediments of Pliocene age are composed of calcareous sandstones and Limestones. Several distortion lines, such as faults, breaks, and some folds striking N–S and NW–SE, that affect El Fayoum Depression are dominant at the peripheries of the depression (El-Sayed et al. 2015). Based on a detailed analysis of the available lithological data, geological map and lithological succession were constructed (Fig. 2b, c).

The surface water hydrology system is represented by the Nile River, irrigation canals, and drains. The area gets irrigation water from the River Nile and the main irrigation branches Bahr Youssef and Bahr Hassan Wassef canals to the depression. Generally, three groundwater aquifers were distinguished in El Fayoum Depression (Mohamed et al. 2015) namely, the Quaternary aquifer, Eocene aquifer, and Nubian sandstone aquifer. Quaternary aquifer is a perched water table aquifer that is maintained by infiltration from canals, drains, and irrigated fields. Many of the springs in El Fayoum depression have their sources from the Quaternary aquifer. Beneath this aquifer, the Eocene aquifer, that is composed of limestone and marls, has high salinity and is therefore unsuitable for potable or irrigation use. The Nubian aquifer is composed of sandstones and shales of Cretaceous

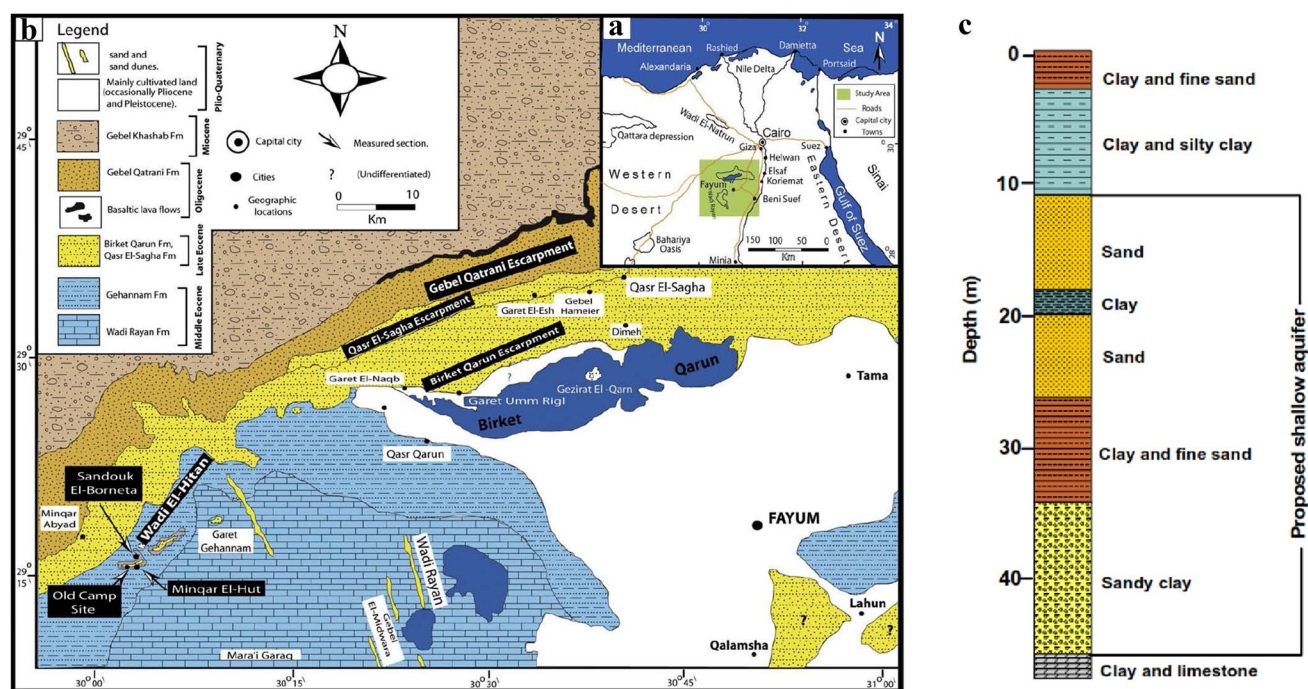


Fig. 2 **a** Location map of El Fayoum depression, Egypt. **b** Geological map of El Fayoum and its adjacent area (Nile valley and northward to the greater Cairo), compiled and modified after Beadnell (1905) and

Said (1962). **c** Lithological succession with the location of proposed shallow aquifer at the center of the depression. Redrawn and modified after Metwaly et al. (2010)

age and it was very deep aquifer (> 1000 m), not exposed in the area of study but reported in the subsurface at Wadi El Rayan and in numbers of oil wells drilled in some localities close to the study area. The Nubian formation is generally characterized by relatively high hydrostatic pressure (Himida and Abdel Baki 1983). The Quaternary aquifer has its maximum thickness (about 60 m) at the center of the depression while, the minimum thickness is less than 1 m along the depression peripheries due to local faulting (Ahmed, 2012). The groundwater depths varied from few centimeters to 9.1 m, with groundwater level ranges from +20 m (amsl) in the area near Nile River to -50 m (bmsl) near Qarun Lake. In addition, the ground-water flows from SE to N and NW in concordance with the general slope of the depression topography in Fig. 1c that shows the land slopes from Lahun to Lake Qarun which occupies the deepest part in El Fayoum depression (Gad and El Hattab 2019). The Quaternary aquifer is thought to be recharged by the seepage from surface irrigation canals, drains, and Nile River. In addition percolation from the underlying fractured limestone of the Eocene aquifer through hydraulic connection (Doerfliger et al. 1999). This study focused on the shallow water-bearing formations of the Quaternary aquifer that directly related to the objective of this investigation.

Materials and methods

sample collection and analysis

A set of representative surface water samples (19 drainage water and 13 canals) and 12 groundwater samples were analyzed for physical measurements including electrical conductivity (EC), pH, temperature, total dissolved solids (TDS), and dissolved oxygen (DO) using portable probes. Chemical parameters comprising major cations (Ca, Mg, Na, K) and anions (Cl, SO_4 , HCO_3) concentrations were also analyzed. All the wells located in El Fayoum depression had been in use during the time of sampling (Fig. 1b). The depths of the selected wells ranged from 8 to 13 m below the surface. The samples were collected in 1-L narrow neck pre-washed polyethylene bottles. Analysis of the water samples was carried out following the methods described in APHA (1995). Total hardness (TH) as CaCO_3 and Ca^{2+} were analyzed using standard EDTA. Mg^{2+} was calculated by taking the differential value between TH and Ca^{2+} concentrations. Na^+ and K^+ were measured using a flame photometer. Total alkalinity and CaCO_3 , CO_3^{2-} , and HCO_3^- were estimated by titrating with HCl. Cl^- was determined by standard Hg (NO_3)₂ titration. SO_4^{2-} and NO_3^- were analyzed using

UV/visible spectrophotometer. All parameters are expressed in milligrams per liter and milliequivalents per liter. Data quality was assessed using the charge balance between the difference of cations and anions (expressed in meq/l) divided by their summation according to the following equation:

$$\Sigma(\text{Cations} - \text{Anions})/\Sigma(\text{Cations} + \text{Anions}) \times 100, \quad (1)$$

With an acceptable range of ± 5 (Hem 1991) that confirm the water quality assessment. Environmental stable isotope ($\delta^{18}\text{O}$ and δD in ‰) samples were collected according to the procedure described in Clark and Fritz (1997). The analysis was done using Picarro L2120-I Isotopic Water Liquid and Vapour Analyzer. Both results were expressed in ‰ (IAEA 1995) with analytical error of ± 0.1 and $\pm 1\%$ for $\delta^{18}\text{O}$ and δD respectively. The stable isotope data are reported in Vienna-Standard Mean Ocean Water (V-SMOW) in ‰ using δ notation according to the equation:

$$\delta = \left[\left(R_{\text{sample}} / R_{\text{standard}} \right) - 1 \right] \times 1000. \quad (2)$$

R_{sample} and R_{standard} are the measured isotopic ratios ($^{18}\text{O}/^{16}\text{O}$) and ($^2\text{H}/^1\text{H}$) of sample and standard material.

Ground surface elevation and the location of the sampling sites were recorded using a global positioning system (GPS) manufactured by GARMIN. This was supported by a topographic sheet made available by the Egyptian Survey Department. Measured and estimated groundwater variables were analyzed within ArcGIS 10.2.2 package. All the chemical and Environmental isotope analyses were carried out in the Central Laboratory of Stable Isotope Hydrology at Egyptian Nuclear and Radiological Regulatory Authority (ENRRA).

Geochemical modeling

The saturation index is a vital geochemical parameter in the fields of hydrogeology and geochemistry, often useful for identifying the existence of some common minerals in the groundwater system (Deutsch 1997). In this present study, saturation indices (SIs) was calculated in terms of the following equation (Lloyd and Heathcote 1985):

$$\text{SI} = \log(\text{IAP}/K_s(T)), \quad (3)$$

where IAP is the relevant ion activity product, which can be calculated by multiplying the ion activity coefficient γ_i and the composition concentration m_i , and $K_s(T)$ is the equilibrium constant of the reaction using the measured sample temperature. When the groundwater is saturated with some minerals, SI equals zero; positive values of SI represent oversaturation, and negative values show undersaturation (Appelo and Postma 1994; Drever 1997). Inverse geochemical modeling with the thermodynamic program PHREEQC (Parkhurst and Appelo 1999) was used to calculate the

geochemical processes responsible for groundwater evolution or changes in quality. To deduce geochemical reactions that accounts for the change in chemical composition of groundwater along the flow path, both aqueous species and saturation indices were calculated. The flow paths were selected on the basis of hydrogeology, hydraulic head variation within the flow system and geographic location in the study area. Minerals used in inverse geochemical modeling are limited to those known to occur in the study area. The mole transfer of minerals and gases reported in mmol kg^{-1} of water. Positive values of phase mole transfers indicate dissolution of minerals or gases, and negative values represent precipitation or outgassing.

Results

General hydrochemistry

Table 1 presents the statistical summary of all the parameters analyzed. The minimum, maximum, mean and standard deviation of the major ions in the Quaternary aquifer of El Fayoum depression compared with WHO (2017) guidelines for drinking water. Temperature of surface water samples (canals, drains) ranged from 20.8 to 26.13 °C with mean of 23.6 °C and 19.46–27.24 °C with mean value of 22.8 °C respectively, while the groundwater ranged between 21.7 and 31.8 °C with mean value of 24.7 °C. The pH values of surface water samples (canals, drains) ranged from 6.16 to 6.7 with mean value of 6.38 and 5.91–7.12 respectively. For groundwater samples the pH values ranged from 5.65 to 6.51 with mean value of 6.09 the data were reflective of slightly acidic to slightly neutral conditions due to that the selected wells were shallow with depth to water ranged from 8 to 13 m, the dissolved carbonates is predominately in HCO_3^- form. In surface water, EC and TDS values exceeded those of groundwater may be due to anthropogenic pollution inputs. The EC of surface water (canals and drains) varied from 606 to 2636 $\mu\text{s/cm}$, with a mean value of 1108 $\mu\text{s/cm}$ and 565 to 3756 $\mu\text{s/cm}$ with a mean value of 1660 $\mu\text{s/cm}$ respectively. In groundwater samples EC values ranged from 162 to 4426 $\mu\text{s/cm}$, with a mean value of 1582 $\mu\text{s/cm}$. TDS values of groundwater samples ranged from 104 to 2832 mg/l exceeding (WHO 2017) standard limits for 50% of collected samples. TDS values ranged from 388 to 1687 mg/l and 361–2431 mg/l in canals and drains samples exceeding (WHO 2017) limits for drinking purposes with 23% and 42% respectively according to (Table 2). According to Konikow and Reilly (1999) and Rhoades et al. (1992) salinity classifications about 42%, 38% of groundwater samples and canal water were slightly saline, while about 42%, 54% of groundwater and canal water were classified

Table 1 Statistical summary of measured physiochemical parameters for groundwater, irrigation canals and drainage water

	pH	EC μS/cm	TDS mg/l	DO mg/l	Temp °C	Major Cations (mg/l)				Major Anions (mg/l)		
						Na ⁺	K ⁺	Mg ²⁺	Ca ²⁺	Cl ⁻	HCO ₃ ⁻	SO ₄ ²⁻
Groundwater												
Min	5.65	514	329	0.00	21.73	53.23	0.50	15	32	53.25	169.80	64.10
Max	6.51	4426	2833	9.03	31.87	429	113	168	144	540	877	863
Mean	6.08	1583	1013	5.59	24.27	159	17.63	61	74.81	161.23	430	242
SD	0.25	1161	743	2.81	2.82	123.9	32.7	48.4	42.64	136.2	259	246.8
Irrigation canals												
Min	6.16	606	388	2.98	21	46.83	4.80	19.20	32	56.80	183.98	58.08
Max	6.70	2636	1687	8.16	26.13	343	14.52	43.50	104	283.99	339.65	577.88
Mean	6.37	1029	659	6.30	23.63	111	8.48	31	54.15	113	246	146
SD	0.20	614	393	1.40	1.92	87.26	3.33	9.35	20.95	80.82	50.88	146.44
Drainage water												
Min	5.91	565	362	3.81	19.46	48	4.84	17.60	32	50	198	56
Max	7.12	3756	2430	11.87	27	702	38	86	208	658	651	1371
Mean	6.36	1607	1030	6.58	23	236	14	47	71.75	206	361	324
SD	0.26	958	617	2.19	1.93	207	9.42	21.87	39	160	140	375

Table 2 Chemical data compared with WHO (2017) guidelines for drinking purposes

Parameters	WHO (2017) Limits	Groundwater (N=12)		Irrigation canals (N=13)		Drainage water (N=19)	
		No. of samples	Percentage %	No. of samples	Percentage %	No. of samples	Percentage %
TDS	1000	6	50	3	23	8	42
Na	200	2	17	2	15	8	42
K	10 ^a	3	25	4	31	7	37
Ca	75 ^a	6	50	3	23	7	37
Mg	30 ^a	7	58	5	38	12	63
Cl	250	1	8	2	15	8	42
SO ₄	500	2	17	1	8	3	16
HCO ₃	300 ^a	7	58	2	15	10	53

^aBased on WHO guidelines (2004)

as fresh respectively. The relative abundance of major cations in shallow groundwater is Na⁺ > Mg²⁺ > Ca²⁺ > K⁺ (on a molar basis) and HCO₃⁻ > Cl⁻ > SO₄²⁻ for anions. For surface water samples (canals and drains) the predominant cations are Na⁺ > Ca²⁺ > Mg²⁺ > K⁺ (on molar basis) and HCO₃⁻ > Cl⁻ > SO₄²⁻ for anions. The maximum Ca²⁺ and Mg²⁺ concentrations of 144 mg/l and 168 mg/l respectively in groundwater samples are however, higher than WHO (2017) standards limits by 50% and 58% respectively. The prevailing common lithology is the old lacustrine deposits which are present within the depression and consist mainly of clay, fine to medium coarse sand with considerable amounts of calcareous and gypsiferous materials. The mean sodium concentrations is 159 mg/l is within the standard limits but potassium concentration is 17.6 mg/l in groundwater samples that exceeds WHO (2004) standards while, for irrigation canals the mean

sodium and potassium concentrations are within WHO standards limits While, for drains Na, K exceeds the international standard as illustrated in Table 2. The presence of HCO₃⁻ ions in shallow groundwater samples is derived from carbon dioxide in the atmosphere, soils and by dissolution of carbonate rocks. Bicarbonate ion represents the first dominant anion in the study area. Most Cl⁻ in the groundwater related to lacustrine deposits found in quaternary aquifer of El Fayoum depression. The most extensive and important occurrences of sulphate ions in the investigated area are sedimentary rocks such as gypsum (CaSO₄·2H₂O) and anhydrite (CaSO₄) that give the chance for active dissolution, leaching and ion-exchange processes. This dominates in the central and western parts of the depression. Further addition of sulphate to groundwater comes from breakdown of organic matter in the soil,

and from addition of leachable sulphate in fertilizers of intensively cultivated area in the depression.

Hypothetical salt combination could classify the hydro-chemical data into three groups as follow:

Group I include salts of [(NaCl, Na₂SO₄, MgSO₄, Mg (HCO₃)₂ and Ca (HCO₃)₂] most of water samples belong to this group (92% groundwater, 85% Irrigation canals and 89% of drainage water).

Group II include salts of [(NaCl, Na₂SO₄, NaHCO₃, Mg (HCO₃)₂ and Ca (HCO₃)₂] some of water samples belong to this group (17% groundwater and 5% of drainage water).

Group III include salts of [(NaCl, Na₂SO₄, MgSO₄, CaSO₄ and Ca (HCO₃)₂] lower numbers of water samples belong to this group (8% of Irrigation canals and 5% of drainage water).

As indicated by the spatial distribution maps of salinity (Fig. 3), The TDS increases from the peripheries that dissected by drains towards the central part of the study area, where the seepage from drains leads to groundwater salinization. Higher TDS values may be related to water–rock interaction, upward recharge from the underlying fracture limestone of Eocene aquifer, irrigation return flow and seepage from the surrounded drains (El-Sheikh 2004). Low TDS values may be attributed to refreshment from irrigation canals.

Discussion

Processes controlling major solutes distribution

The rock dominance of the major ion chemistry in the study area provides an insight of chemical weathering in the aquifer, since weathering of different parent rocks

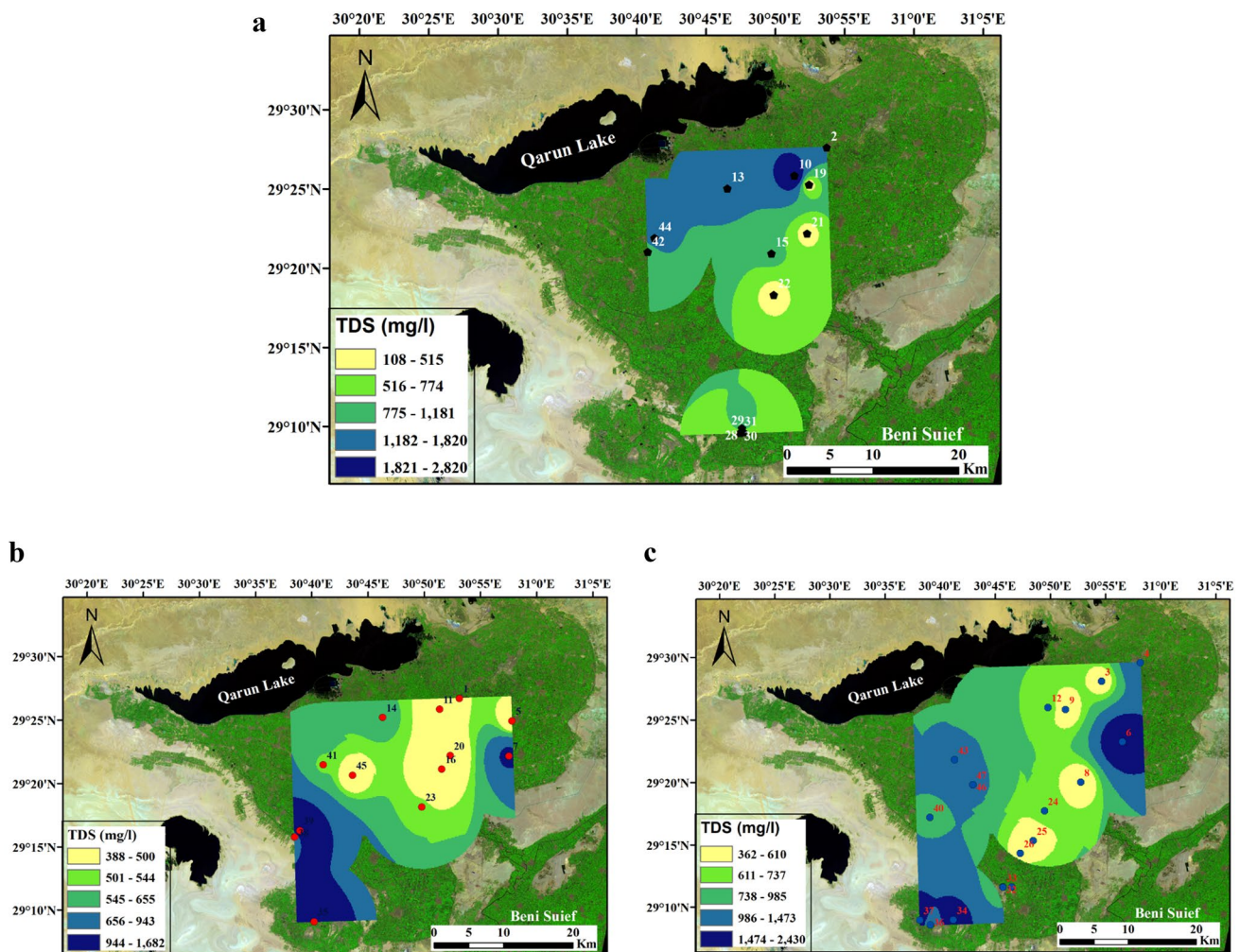


Fig. 3 Total dissolved solids distribution maps for a groundwater, b irrigation canals, c drainage water

(e.g., carbonates, silicates and evaporites) yield different combinations of dissolved cations and anions to solution. The Gibbs diagram is widely used to study the relationship between water chemistry and aquifer lithology (Gibbs 1970). The functional sources of the dissolved chemical constituents can be divided into three distinct fields in this

diagram, namely rainfall dominance, evaporation dominance and rock-weathering dominance areas. The ratios of $Cl / (Cl + HCO_3)$ and $(Na + K) / (Na + K + Ca)$ as a function of TDS were drawn in Fig. 4. The majority of the samples fell in evaporation-dominated field demonstrating the

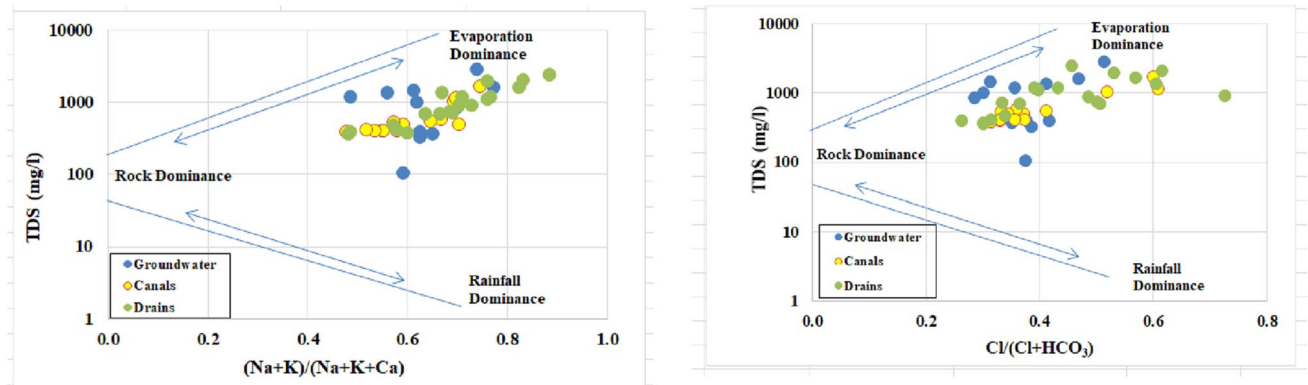


Fig. 4 Gibbs diagram for cations and anions in (meq/l) of collected water samples

Table 3 Calculated ionic ratios in (meq/l) for the collected water samples

Sample no.	Na/Cl	Ca/Mg	Ca/SO ₄	Sample no.	Na/Cl	Ca/Mg	Ca/SO ₄
Groundwater				Drainage water			
2	1.207	1.706	1.325	3	1.589	1.200	1.326
10	1.227	0.486	0.563	4	1.195	1.255	0.680
13	1.457	0.542	0.963	6	3.394	0.567	0.178
15	1.749	0.538	1.261	8	1.550	0.667	1.168
19	1.342	0.800	1.194	9	1.486	1.500	2.069
21	1.444	1.000	1.127	12	1.829	0.462	0.676
22	2.013	1.352	1.063	24	1.661	0.778	0.883
28	3.280	1.200	0.267	25	1.486	1.000	0.964
29	1.417	0.771	1.095	26	1.888	1.599	1.257
30	1.500	0.800	1.053	27	1.271	0.571	1.036
31	1.155	1.000	1.274	32	1.386	1.400	0.918
42	1.805	1.023	1.157	33	1.408	1.167	0.805
44	1.000	0.560	1.028	34	1.772	1.273	0.579
Irrigation canals				36	1.648	1.818	0.458
1	2.191	1.259	1.138	37	2.081	0.750	0.258
7	1.432	1.102	0.784	40	1.570	0.875	0.638
14	1.431	0.556	1.031	43	1.664	0.769	0.909
16	1.300	0.667	1.000	46	1.984	0.840	0.676
20	1.275	1.500	1.983	47	1.569	0.700	1.407
23	1.477	1.000	1.290				
35	1.231	1.111	0.701				
38	1.608	1.500	1.290				
39	1.864	1.444	0.432				
41	1.591	1.061	1.489				
45	1.444	1.000	1.515				
5	1.356	1.652	1.487				
11	1.178	1.045	1.267				

Bold values were < 1

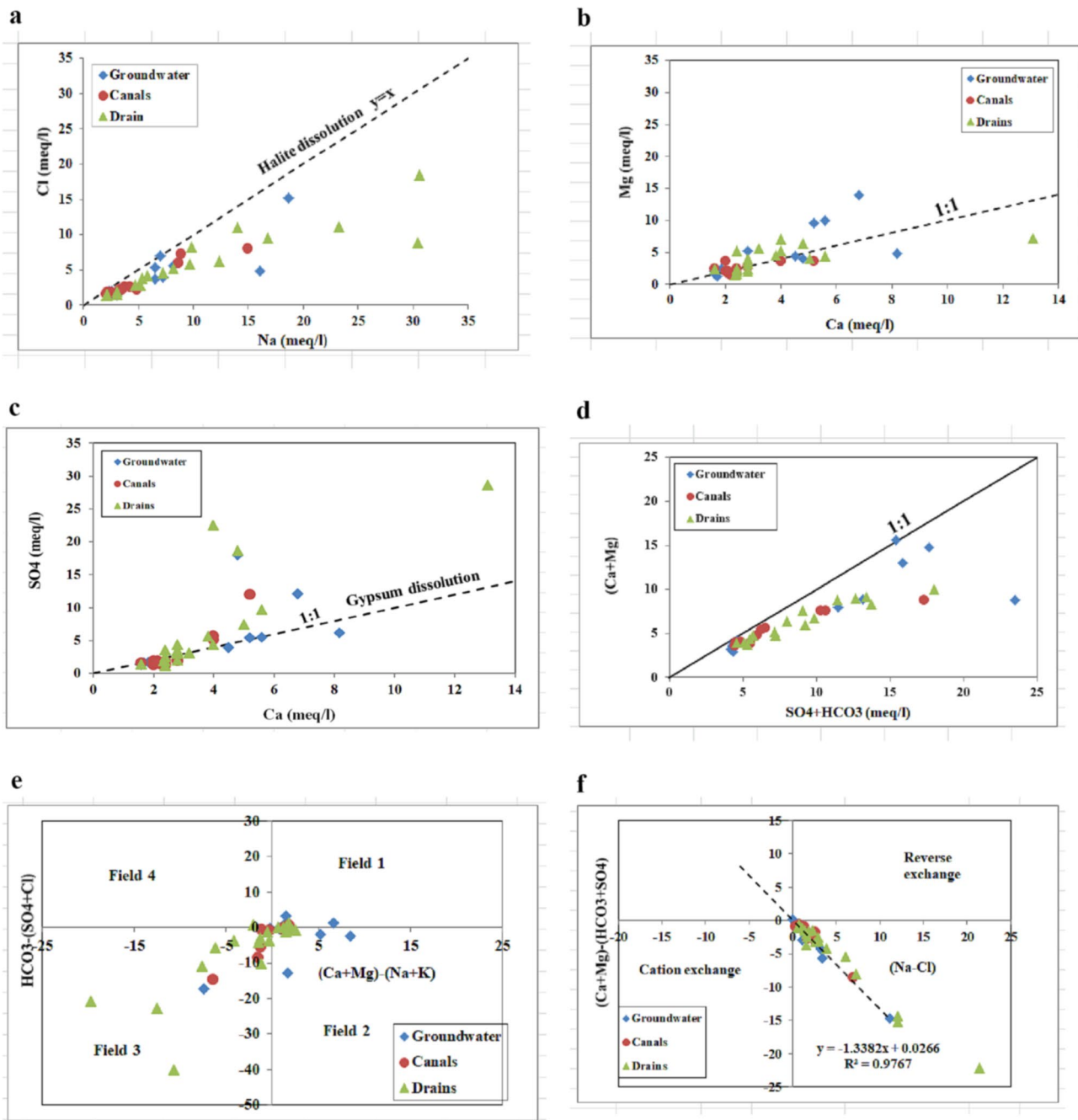


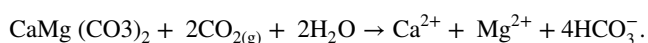
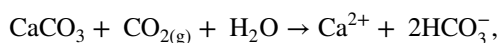
Fig. 5 Relationships of **a** Na^+ vs. Cl^- , **b** Ca^{2+} vs. Mg^{2+} , **c** Ca^{2+} vs. SO_4^{2-} , **d** Cl^- vs. $(\text{Ca}^{2+} + \text{Mg}^{2+})$, **e** Chadha's plot, **f** $(\text{Ca}^{2+} + \text{Mg}^{2+}) - (\text{SO}_4^{2-} + \text{HCO}_3^-)$ vs. $(\text{Na}^+ - \text{Cl}^-)$ in (meq/l) for collected water samples in the study area

importance of irrigation return flow on collected surface and groundwater samples chemistry.

According to (Table 3) for calculated ionic ratios and (Fig 5a) the Na^+/Cl^- showed clear enrichment of Na^+ in the surface (canals and drains) and groundwater samples. The $\text{Na}^+ / \text{Cl}^-$ ratios in the study area varied from 1 to 3.3 with an average value of 1.6 in groundwater and for surface water, it varied from 1.2 to 2.2 in canals and 1.2 to 3.4 in drains. In general, the Na^+

Cl^- molar ratio should be approximately equal to 1, if the halite dissolution is the only source. The majority of the samples (Fig 5a) having a higher Na^+/Cl^- ratio suggested another possible source of Na^+ may be ion-exchange or silicate weathering be responsible for the exceeding of Na^+ concentration in collected water samples. The $\text{Ca}^{2+}/\text{Mg}^{2+}$ ratio suggests that dissolution of calcite and dolomite in the aquifer. Results of surface and groundwater samples ratios (Fig 5b) ranged between 0.49 and

1.71 with an average value of 0.93 for groundwater and from 0.56 to 1.65 with an average value of 1.14 and 0.46 to 1.82 with an average value of 1.02 for canal and drain water samples respectively. That is, if the ratio $Ca/Mg=1$, dissolution of dolomite should occur, whereas a higher ratio is indicative of greater calcite contribution (Maya and Loucks 1995). For groundwater samples, about 54% have $Mg>Ca$ and 46% have $Ca>Mg$ according to (Table 3) indicative of dissolution of calcite /dolomite minerals that largely controlled by CO_2 fugacity and pH according to the reactions:



Drainage water samples show more abundance of $Mg>Ca$ by 53% than only 15% for canals water. Ca^{2+}/SO_4^{2-} ratio illustrated in Fig 5c showed that drainage water samples have an excess SO_4^{2-} over Ca^{2+} in about 68% of samples compared with 23% and 24% in groundwater and canals water, respectively that may be due to gypsum dissolution effect. The plot of $(Ca^{2+} + Mg^{2+})$ vs. $(SO_4^{2-} + HCO_3^-)$ (Fig.5d) shows that all surface and groundwater samples are distributed close to or below 1:1 line due to an excess of $(SO_4^{2-} + HCO_3^-)$ over $(Ca^{2+} + Mg^{2+})$ an indication of that the dissolution of calcite, dolomite, anhydrite and gypsum are the dominant reactions and ion exchange tends to be predominant process in the system (McLean and Jankowski 2000).

Chadha's diagram can be used to study the various hydrochemical processes responsible for water system evolution such as base cation exchange, mixing of natural waters and saline water (Chadha 1999). Results of hydrochemical analysis

plotted on this diagram (Fig 5e) show that some groundwater samples can be related to field 1 of (Ca-Mg- HCO_3 water type) and drains are related to field 2 of (Ca-Mg- SO_4/Cl mixed water) and the rest of samples related to field 3 (Na-Cl water type). To check the hypothesis of cation exchange is one of geochemical process that may control water chemistry, The relation of $(Ca^{2+} + Mg^{2+}) - (SO_4^{2-} + HCO_3^-)$ vs. $(Na^+ - Cl^-)$ meq/l was illustrated in Fig 5f can better indicate the involvement of cation exchange between groundwater and its host environment. Negative values of $(Ca^{2+} + Mg^{2+}) - (SO_4^{2-} + HCO_3^-)$ are usually used to demonstrate the involvement of cation exchange, inducing the ions absorbed on the surface of fine-grained materials of the aquifer to be replaced by the ions in the solutions. The ratio of this trend in surface and groundwater samples was linear with a slope of -1.33 and the correlation coefficient was 0.97. As the cation exchange between Na^+ and Ca^{2+} or Mg^{2+} will lower the concentration of Ca^{2+} dissolved in water, this was illustrated in the relation between Ca^{2+} and SO_4^{2-} in Fig 5c.

Geochemical modeling

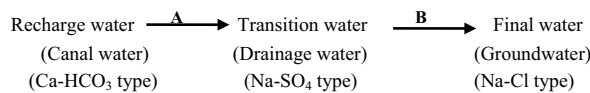
In order to evaluate possible hydrochemical reactions along the flow paths, inverse mass-balance models were developed using the PHREEQC program (Parkhurst and Appelo 1999). Three geochemical processes may contribute to generation of solutes in groundwater including evaporation, carbonate dissolution /precipitation and silicate weathering (Garrels and MacKenzie 1971). Statistical summary of thermodynamic speciation calculations for surface and groundwater samples using PHREEQC program were illustrated in Table 4. The results indicated that the surface (canals, drains) and groundwater samples of the Quaternary aquifer

Table 4 Statistical summary of saturation indices calculation using PHREEQC

	Al(OH) ₃	Anhydrite CaSO ₄	Aragonite CaCO ₃	Barite BaSO ₄	Calcite CaCO ₃	CO ₂ (g)	Dolomite CaMg(CO ₃) ₂	Gibbsite Al(OH) ₃	Goethite FeOOH	Gypsum CaSO ₄ ·2H ₂ O	Hematite Fe ₂ O ₃
Groundwater											
Min	-1	-2.82	-2.28	0.76	-2.14	-1.21	-4.28	1.69	2.83	-2.12	7.02
Max	0.88	-1.1	-0.79	1.8	-0.65	0.06	-1.07	3.58	6.23	-0.91	14.98
Mean	-0.093	-1.911	-1.390	1.141	-1.245	-0.664	-2.269	2.637	4.506	-1.647	10.951
SD	0.529	0.500	0.435	0.361	0.436	0.468	0.967	0.514	0.895	0.426	1.994
Irrigation canal											
Min	0.11	-2.28	-1.58	0.77	-1.44	-1.47	-2.75	2.69	4.33	-2.05	10.69
Max	1.98	-1.21	1.2	1.9	-0.67	-0.8	-1.3	4.66	7.26	-0.98	16.28
Mean	0.97	-2.115	-1.39	1.05	-1.245	-1.025	-2.37	3.67	6.025	-1.89	14.05
SD	0.428	0.344	0.765	0.309	0.258	0.187	0.503	0.447	0.775	0.346	1.540
Drainage water											
Min	0.49	-2.34	-1.53	1.01	-1.38	-1.42	-2.87	3.2	4.98	-2.11	11.81
Max	1.85	2.24	-0.2	1.75	-0.05	1.27	0.22	4.52	8.6	-0.45	18.97
Mean	1.113	-1.244	-1.103	1.276	-0.941	-0.748	-1.781	3.823	6.335	-1.482	14.519
SD	0.321	1.276	0.337	0.211	0.342	0.582	0.710	0.319	0.880	0.425	1.758

were-undersaturated (dissolution is required to achieve equilibrium) with minerals and gases in order of Al (OH)₃ > partial pressure of CO_{2(g)} > Calcite CaCO₃ > Aragonite CaCO₃ > Gypsum CaSO₄·2H₂O > Anhydrite CaSO₄ > Dolomite CaMg (CO₃)₂ with the mean SI values of (−0.093, −0.664, −1.245, −1.390, −1.647, −1.911 and −2.269 respectively. Negative values of PCO_{2(g)} may reflect the recharge from underlying aquifer and seepage from drains. Surface and groundwater samples have a tendency to precipitate the minerals/gases in order of Hematite Fe₂O₃ > Goethite FeOOH > Gibbsite Al (OH)₃ > Barite BaSO₄ with the mean values of SI of 10.951, 4.506, 2.637 and 1.141 respectively.

Two flow paths were modeled based on Hydrochemical data as illustrated in Fig. 1b, the flow path (A) at which the less mineralized (recharge water) was canal water (sample 20) which has TDS value of 388 mg/l and the moderate mineralized (transition water) one was drainage water (sample 6) which has TDS value of 2431 mg/l. The flow path (B) at the moderate mineralized drainage water (sample 6) also modeled with the more mineralized (Final water) groundwater sample (sample 10) which has TDS value of 2833 mg/l.



The inverse modeling in PHREEQC takes into account uncertainty limits that are constrained to satisfy the mole balance for each element and valence state as well as the charge balance for each solution within the simulation. The simulations were constrained within the specified uncertainty limits (0.025 or 0.05) as default for all model runs. Potential phases in the inverse modeling were selected based on (precipitation/dissolution) results from hydrochemical data and saturation index calculations for the modeled samples (Table 5). The results of inverse geochemical modeling were illustrated in Table 5 as shown below: 26 and 14 models were resulted for flow paths A, B respectively with selection done based on the lowest sum of residuals and uncertainty limits. The inverse model was constrained so the primary mineral phase including calcite, aragonite, anhydrite and gypsum with carbon dioxide (gas) are constrained to dissolve until they reach saturation, Whereas H_{2(g)}, hydrogen sulphide (gas) and O_{2(g)} are constrained to out gassed in all models for flow path (A). For flow

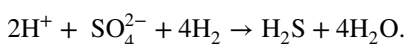
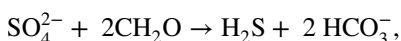
Table 5 Inverse modeling along the flow paths A, B (Inverse model calculations were conducted using PHREEQC v.214.03 computer program (Parkhurst and Appelo 1999). Thermodynamic database

used: phreeq.dat values are in mol/kg H₂O. Positive (mass entering water) and negative (mass leaving water) phase mole transfers indicate dissolution and precipitation, respectively, as mmol kg^{−1})

Mineral	Flow path A: phase mole transition (mol/kg H ₂ O)			
Phases	Canal water (20) → Drainage water (6)			
Calcite	1.70E−03	−	−	−
Aragonite	−	1.70E−03	−	−
Anhydrite	−	−	1.70E−03	−
Gypsum	−	−	−	1.70E−03
CO _{2(g)}	9.59E−03	9.59E−03	1.13E−02	1.13E−02
H _{2(g)}	−7.03E+01	−7.03E+01	−7.03E+01	−7.03E+01
H ₂ S(g)	−3.24E−03	−3.24E−03	−4.94E−03	−4.94E−03
O _{2(g)}	−3.52E+01	−3.52E+01	−3.52E+01	−3.52E+01
Mineral	Flow path B: phase mole transition (mol/kg H ₂ O)			
Phases	Drainage water (6) → groundwater (10)			
Calcite	2.70E−03	−	−	−
Dolomite	−	−	−	2.70E−03
Aragonite	−	2.70E−03	−	−
Anhydrite	−	−	2.70E−03	−
Gypsum	−	−	−	2.70E−03
CO _{2(g)}	−1.28E−02	−1.28E−02	−1.01E−02	−1.55E−02
H _{2(g)}	−1.80E+01	−1.80E+01	−1.80E+01	−1.80E+01
H ₂ S(g)	7.13E−03	7.13E−03	4.43E−03	9.83E−03
O _{2(g)}	−8.97E+00	−8.97E+00	−8.98E+00	−8.97E+00

path (B), Dolomite, Anhydrite and Gypsum are tend to dissolve with Carbon dioxide (gas), $H_{2(g)}$ and $O_{2(g)}$ gases tend to precipitate.

The Quaternary deposits cover wide stretches of the investigated area are distinguished into Holocene deposits and Pleistocene deposits as mentioned in El-Sheikh (2004). The old lacustrine deposits (45 m thick) formed the Pleistocene deposits composed mainly of clay fine to medium coarse sand with considerable amounts of calcareous and gypsiferous materials. As carbonate minerals (calcite, dolomite) dissolution for both flow paths A, B contribute to Ca^{2+} , Mg^{2+} and HCO_3^- and Gypsum dissolution leads an increase in Ca^{2+} and SO_4^{2-} to the system. Additional increase in Ca^{2+} leads to dissolution of more calcite that increase CO_2 , which leads to slightly lower pH as illustrated in Table 1. The out gassing of hydrogen sulphide is occurring in flow path A, which an indication of SO_4^{2-} reduction. Sulphate reduction occurs extensively in natural systems that involves the consumption of substantial amounts of hydrogen ions and production of HS^- at certain pH. As drainage water contains organic carbon or H_2 that is oxidized while sulphate is reduced (Canfield 2001) according to the following equations:



The hydrogen ions are consumed and bicarbonate is produced, which leads to an increase in PH as shown in Table 1 for drainage water samples. Field measured ORP (oxidation – reduction potential) for drainage water have ranged between (–64 to 611 mv) while it was ranged between (227–767 mv) and (125–551 mv) for groundwater and irrigation canals respectively. (El Mahllawy et al. 2013) studied the composition and activation aspects of El Fayoum clays for use as a drilling fluid, the mineralogical analysis of the studied samples using XRD (X-Ray Diffraction) were essentially montmorillonite, kaolinite and illite as clay minerals in a descending order of abundance. Quartz and calcite minerals were also found in minor amounts as non-clay components.

Inverse model calculations were conducted using PHREEQC v.214.03 computer program (Parkhurst and Appelo 1999). Thermodynamic database used: phreeq.dat values are in mol/kg H_2O . Positive (mass entering water) and negative (mass leaving water) phase mole transfers indicate dissolution and precipitation, respectively, as $mmol\ kg^{-1}$.

Environmental isotope studies

Isotopic composition of surface and groundwater samples

Stable isotopes composition ($\delta^{18}O$ and δD) of 44 surface and groundwater samples were measured to provide basic

information on the origin and sources of recharge for the Quaternary aquifer in the studied area. The stable isotope composition of surface and groundwater samples collected together with those of the d-excess values is compiled in Table 6. Groundwater values of $\delta^{18}O$ range between (+3.17 and +4.21 ‰) with an average value of 3.84‰ and δD values fall or lie between (+25.41 and +32.31 ‰) with an average value of 29.53 ‰ and d-excess values range from (–2.15 to 0.14 ‰).

For surface water (canals, drains) samples, $\delta^{18}O$ values range from +4.03 to 4.83‰ and +4 to +5.19‰, while δD values range from +30.75 to +34.91‰ and +28.6 to +35.57‰ with d-excess values fall between (–3.73 to –0.95‰) and (–5.95 to –2.18‰) respectively. The plot of $\delta^{18}O$ and δD (Fig. 6) offers a complementary insight into the origin of groundwater in El Fayoum depression according to their isotopic compositions and to their position regarding GMWL (Global Meteoric Water Line) (Craig 1961). The global meteoric water line (GMWL) represents the regression line of global continental precipitation samples with the following equation (Craig 1961): $\delta D = 8 \delta^{18}O + 10$, with a slope of 8 and intercept 10. The plot of $\delta^{18}O$ versus δD in ‰ surface and groundwater samples (Fig. 6) illustrate that all collected water samples are located within an evaporation line given by a regression equation of slope 6.63 and intercept of 3.98. An enrichment occurs for both $\delta^{18}O$ and δD values compared with Nile River revealing the occurrence of intensive evaporation process in addition to irrigation return phenomena with an increase of salinity as shown in Fig. 7 for TDS in (mg/l) and $\delta^{18}O$ in ‰.

TDS values in Fig. 7 show an increment compared with slightly constant values of $\delta^{18}O$ for collected water samples. This may be due to evaporation and dissolution processes that affect surface and groundwater samples in El Fayoum depression.

Conclusions

The results of this study showed that integration of hydrochemical data, inverse geochemical modeling coupled with isotopic data can help to understand the hydrogeochemical processes controlling water chemistry evolution in El Fayoum depression. The relative abundance of major cations in shallow groundwater is $Na^+ > Mg^{2+} > Ca^{2+} > K^+$ (on molar basis) and $HCO_3^- > Cl^- > SO_4^{2-}$ for anions. For surface water samples (canals and drains) the predominant cations are $Na^+ > Ca^{2+} > Mg^{2+} > K^+$ (on molar basis) and $HCO_3^- > Cl^- > SO_4^{2-}$ for anions. Gibbs plot that illustrate Rock-water interaction which affects Quaternary aquifer system indicates that most water samples fall in evaporation

Table 6 Stable isotope composition for collected surface and groundwater samples

Sample no.	$\delta\text{O-18}$ ‰	δD ‰	d-excess ‰	Sample no.	$\delta\text{O-18}$ ‰	δD ‰	d-excess ‰
Groundwater				Drainage water			
2	4.05	30.25	-2.15	3	4.34	31.81	-2.91
10				4	4.47	32.82	-2.94
13	3.17	25.5	0.14	6			
15	3.68	28.46	-0.98	8	4.33	31.94	-2.7
19	4.15	32.15	-1.05	9	4.35	32.36	-2.44
21	4.21	32.31	-1.37	12	4.2	31.33	-2.27
22	4.03	30.69	-1.55	24	4.35	31.27	-3.53
28	3.71	28.56	-1.12	25	4.2	30.93	-2.67
29	4.13	31.14	-1.9	26	4.2	31.42	-2.18
30	4.14	31.43	-1.69	27	4.41	32.03	-3.25
31	4.08	30.94	-1.7	32	4.62	33.52	-3.44
42	3.73	28.89	-0.95	33	4.52	32.59	-3.57
44	3.3	25.41	-0.99	34			
Irrigation canals				36	5.19	35.57	-5.95
1	4.32	31.45	-3.11	37	4.74	33.34	-4.58
7	4.37	31.93	-3.03	40	4.49	33.72	-2.2
14	4.03	31.29	-0.95	43	4	28.66	-3.34
16	4.23	31.77	-2.07	46	4.3	30.41	-3.99
20	4.2	32.27	-1.33	47	4.48	32.17	-3.67
23	4.26	30.75	-3.33	Nile River	2.3	23.4	5
35	4.65	33.92	-3.28	Nile before high dam (Aly et al 1993)	-0.6	4.3	9.1
38	4.35	32.64	-2.16				
39	4.83	34.91	-3.73				
41	4.25	32.05	-1.95				
45	4.51	32.4	-3.68				

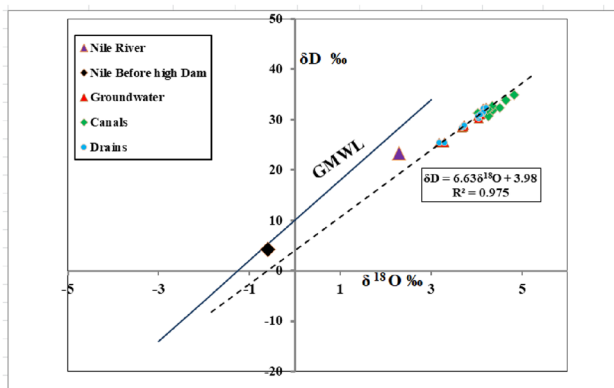


Fig. 6 $\delta^{18}\text{O}$ versus δD in ‰ for collected water samples

dominant zone. As Nile River being the only recharge source for the depression via Bahr Youssef, the groundwater in the study area is characterized by Na-Ca-Mg/HCO₃ type in 92%, while irrigation canals and drainage water have this type 77%, 58% respectively. The concentration of (SO₄²⁻ + HCO₃⁻) exceeds (Ca²⁺ + Mg²⁺), which is the result of calcite,

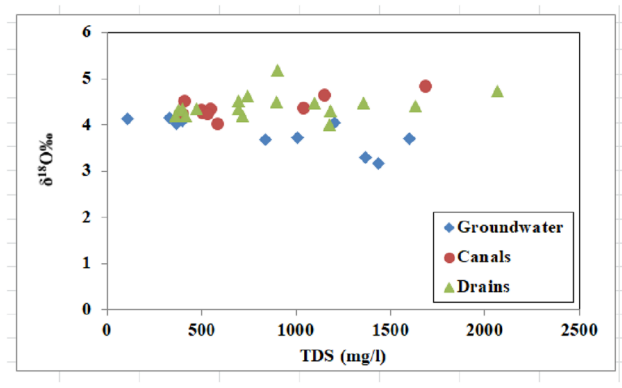


Fig. 7 TDS in (mg/l) vs. $\delta^{18}\text{O}$ in ‰ for collected water samples

dolomite in the system. Gypsum dissolution contributes to increase of both Ca²⁺ and SO₄²⁻ in the aquifer, which leads to a slightly low PH and supersaturation or near equilibrium of calcite. Na⁺ is comparatively higher than Cl⁻ for surface and groundwater samples suggested cation-exchange process that

greatly affects groundwater ion compositions through interaction between water and aquifer materials. Saturation Index using PHREEQC software results indicated that the surface (canals, drains) and groundwater samples were-undersaturated (dissolution is required to achieve equilibrium) with minerals and gases in order of $\text{Al}(\text{OH})_3 >$ partial pressure of $\text{CO}_{2(\text{g})} >$ Calcite $\text{CaCO}_3 >$ Aragonite $\text{CaCO}_3 >$ Gypsum $\text{CaSO}_4 \cdot 2\text{H}_2\text{O} >$ Anhydrite $\text{CaSO}_4 >$ Dolomite $\text{CaMg}(\text{CO}_3)_2$. Negative values of $\text{PCO}_{2(\text{g})}$ may reflect the recharge from underlying aquifer and seepage from drains. Surface and groundwater samples have a tendency to precipitate the minerals/gases in order of Hematite $\text{Fe}_2\text{O}_3 >$ Goethite $\text{FeOOH} >$ Gibbsite $\text{Al}(\text{OH})_3 >$ Barite BaSO_4 . The inverse geochemical modeling demonstrated that dissolution of carbonate (calcite, dolomite) and evaporites (gypsum, Anhydrite) minerals with outgassing of hydrogen sulphide as a result of organic matter reduction and microbial processes. Cation-exchange of Ca^{2+} over Na^+ also important geochemical processes in the aquifer system of the area. Environmental stable isotope data revealed that all surface and groundwater samples have enriched values of $\delta^{18}\text{O}$ and δD compared with Nile River revealing the occurrence of intensive evaporation process in addition to irrigation return phenomena that effects on salinity as illustrated for TDS in (mg/l) and $\delta^{18}\text{O}$ in ‰ relationship. Finally, from literature review and field observations, an environmental protection is needed through continuous monitoring of water resources quantity and quality with the possibility of contamination removal and construct sanitation network extends to all regions of El Fayoum depression.

Supplementary Information The online version contains supplementary material available at <https://doi.org/10.1007/s12665-022-10192-4>.

Funding Open access funding provided by The Science, Technology & Innovation Funding Authority (STDF) in cooperation with The Egyptian Knowledge Bank (EKB).

Open Access This article is licensed under a Creative Commons Attribution 4.0 International License, which permits use, sharing, adaptation, distribution and reproduction in any medium or format, as long as you give appropriate credit to the original author(s) and the source, provide a link to the Creative Commons licence, and indicate if changes were made. The images or other third party material in this article are included in the article's Creative Commons licence, unless indicated otherwise in a credit line to the material. If material is not included in the article's Creative Commons licence and your intended use is not permitted by statutory regulation or exceeds the permitted use, you will need to obtain permission directly from the copyright holder. To view a copy of this licence, visit <http://creativecommons.org/licenses/by/4.0/>.

References

- Abdel Kawy W, Belal A (2012) Spatial analysis techniques to survey the heavy metals content of the cultivated land in El-Fayoum depression. *Egypt Arab J Geosci* 5:1247–1258
- Ahmed MA (2012) Assessment of intrinsic vulnerability to contamination for the alluvial aquifer in El Fayoum Depression using DRASTIC Method. *J Radiat Res Appl Sci* 5(4):743–768
- Aly AIM, Froehlich K, Nada A, Awad M, Hamza M, Salem WM (1993) Study of Environmental isotope distribution in the Aswan High Dam Lake (Egypt) for estimation of evaporation lake water and its recharge to adjacent groundwater. *Environ Geochem Health* 15(1):37
- American Public Health Association (APHA) (1995) AWWA (American Water Works Assoc.); WPCF (Water Poll. Contr. Fed.) Standard methods for the examination of water and waste water, 13th edn. Am. Public Health Assoc, Washington, DC, p 874
- Apodaca LE, Jeffrey BB, Michelle CS (2002) Water quality in shallow alluvial aquifers, Upper Colorado River Basin, Colorado, 1997. *J Am Water Res Assoc* 38(1):133–143
- Appelo CAJ, Postma D (1994) *Geochemistry groundwater and pollution*. AA Balkema, Rotterdam
- Beadnell HJL (1905) The topography and geology of the Fayoum Province of Egypt. Survey Department of Egypt, Cairo, p 101
- Berihu BA, Ugur DE, Mehmet C (2017) Assessment of hydrogeochemistry and environmental isotopes of surface and groundwaters in the Kutahya Plain, Turkey. *J Afr Earth Sci* 134:230–240
- Canfield DE (2001) Isotope fractionation by natural populations of sulfate-reducing bacteria. *Goechim Cosmochim Acta* 65(7):1117–1124
- Chadha DK (1999) A proposed new diagram for geochemical classification of natural waters and interpretation of chemical data. *Hydrogeol J* 7:431–439. <https://doi.org/10.1007/s100400050216>
- Clark ID, Fritz P (1997) *Environmental Isotopes in hydrogeology*. Lewis Publisher, New York
- Craig H (1961) Isotopic variations in meteoric waters. *Science* 133:1702–1703
- Deutsch WJ (1997) *Groundwater geochemistry: fundamentals and applications to contamination*. CRC Press, Boca Raton
- Doerfliger N, Jeannin PY, Zwahlen F (1999) Water vulnerability assessment in karst environments: a new method of defining protection areas using a multi-attribute approach and GIS tools (EPIK method). *Environ Geol* 39:165–176
- Drever JI (1997) *The geochemistry of natural waters: surface and groundwater environments*. Prentice Hall, New Jersey
- El Mahllawy MS, Sharara AM, Hassaan MM, Abdel Haleem AM (2013) The composition and activation aspects of El Fayoum clays for using as a drilling fluid. *Egypt J Pet* 22:395–404
- El Sayed SA, Moussa EMM, El-Sabagh MEI (2015) Evaluation of heavy metal content in Qaroun Lake, El Fayoum, Egypt. Part I: bottom sediments. *J Radiat Res* 8:276–285. <https://doi.org/10.1016/j.jrras.2015.02.011>
- El-Sheikh AE (2004) Water budget analysis of the quaternary deposits for the assessment of the water logging problem in El Fayoum depression. Ph.D. Thesis, Fac. of Science, Al-Azhar University
- Fontes JC (1980) Environmental isotopes in groundwater hydrology. In: Fritz P, Fontes JC (eds) *Handbook of environmental isotope geochemistry*. Elsevier, Amsterdam, pp 75–140
- Gad M, El Hattab M (2019) Integration of water pollution indices and DRASTIC model for assessment of groundwater quality in El Fayoum Depression, western desert Egypt. *J Afr Earth Sci* 158:103554. <https://doi.org/10.1016/j.jafrearsci.2019.103554>
- Gad A, El-Zeiny A (2016) Spatial analysis for sustainable development of El Fayoum and Wadi El Natrun Desert Depressions, Egypt with the aid of remote sensing and GIS. *Environ Earth Sci* 8(3):1–18. <https://doi.org/10.9734/IJGEESI/2016/29706>
- Garrels RM, MacKenzie FT (1971) *Evolution of sedimentary rocks*. Norton, New York
- Gat JR (1981) Groundwater. In: Gat JR, Gonfiantini R (eds) *Stable isotope hydrology*. IAEA, Vienna, pp 223–240

- Gibbs RJ (1970) Mechanisms controlling world water chemistry. *Science* 170:1088–1090
- Gupta G, Abd El-Hamid Z (2003) Water quality of Lake Qarun, Egypt. *Int J Environ Stud* 60:651–657
- Hem JD (1991) Study and interpretation of the chemical characteristics of natural water, 3rd edn. Scientific Publication, Jodhpur, p 2254
- Himidi IH, Abdel Baki AA (1983) Hydrogeological conditions of El Fayoum and Wadi El Rayan depressions A.R.E. *Ann Geol Surv Egypt* 10:837–853
- Hussein HA, Ricka A, Kuchovsky T, El Osta MM (2017) Groundwater hydrochemistry and origin in the south-eastern part of Wadi El Natrun, Egypt. *Arab J Geosci* 10:170–184. <https://doi.org/10.1007/s12517-017-2960-x>
- IAEA (1995) Reference and inter-comparison materials for stable isotopes of light elements. In: Proc. of a consultants meeting held in Vienna, 1-3/10/1993, IAEA, Vienna, TECDOC-825, p 165
- Konikow L, Reilly T (1999). Seawater intrusion in the United States. In: Seawater intrusion in coastal aquifers-concepts, methods and practices. Springer, pp 463–506
- Leontiadias IL, Payne BR, Christodoulou T (1988) Isotope hydrology of the Aghios Nikolaos area of Crete, Greece. *J Hydrol* 98:121–132
- Liu F, Zhao Z, Yang L, Ma Y, Xu Y, Gong L, Liu H (2020) Geochemical characterization of shallow groundwater using statistical analysis and geochemical modeling in an irrigated region along the upper Yellow River, Northwestern China. *J Geochem Explor* 215:106565
- Lloyd JW, Heathcote J (1985) Natural inorganic hydrochemistry in relation to groundwater. Oxford University Press, New York
- Mansour SA, Sidky MM (2002) Ecotoxicological Studies. 3. Heavy metals contaminating water and fish from Fayoum Governorate, Egypt. *Food Chem* 78:15–22
- Mansour SA, Sidky MM (2003) Ecotoxicological Studies. 6. The first comparative study between Lake Qarun and Wadi El-Rayan wetland (Egypt), with respect to contamination of their major components. *Food Chem* 82:181–189
- Maya AL, Loucks MD (1995) Solute and isotopic geochemistry and groundwater flow in the Central Wasatch Range, Utah. *J Hydrol* 172:31–59
- Mclean W, Jankowski J (2000) Groundwater quality and sustainability in an alluvial aquifer, Australia. In: Sililo et al. (ed) Proc. XXX IAH congress on groundwater: past achievements and future challenges, Cape Town, 26th November–1st December 2000. AA Balkema, Rotterdam
- Metwaly M, El-Qady G, Massoud U, El-Kenawy A, Matsushima J, Al-Arifi N (2010) Integrated geoelectrical survey for groundwater and shallow subsurface evaluation: case study at Siliyin spring, El-Fayoum, Egypt. *Int J Earth Sci (geol Rundsch)* 99:1427–1436
- Mgbenu CN, Egbueri JC (2019) The hydrogeochemical signatures, quality indices and health risk assessment of water resources in Umunya district, southeast Nigeria. *Appl Water Sci* 9:22. <https://doi.org/10.1007/s1320.1-019-0900-5>
- Mohamed EA, El-Kammar AM, Yehia MM, Abu Salem HS (2015) Hydrogeochemical evolution of inland lakes' water: a study of major element geochemistry in the Wadi El Raiyan Depression, Egypt. *J Adv Res* 6(6):1031–1044. <https://doi.org/10.1016/j.jare.2014.12.008>
- Murray KS (1996) Hydrology and geochemistry of thermal waters in the Upper Napa valley, California. *Ground Water* 34(6):1115–1124
- Parkhurst DL, Appelo CAJ (1999) User's Guide to PHREEQC (Version 2) A computer program for Speciation, Batch-Reaction, One dimensional Transport, and Inverse Geochemical calculations. United States Geological Survey, Water Resources, Investigations Report 99-4259, Washington, DC, p 326
- Plummer LN (1992) Geochemical modeling of water-rock interaction: past, present, future. In: Kharaka YK, Maest AS (eds) Water-rock interaction. Proc 7th Int. Conf. Balkema, Rotterdam, pp 23–33
- Redwan M, Elhaddad E (2017) Heavy metals seasonal variability and distribution in Lake Qaroun sediments, El Fayoum, Egypt. *J Afr Earth Sci* 134:48–55. <https://doi.org/10.1016/j.jafrearsci.2017.06.005>
- Rhoades JD, Kandiah A, Mashali A (1992) The use of saline waters for crop production. FAO
- Rosen M, Jones S (1998) Controls of the chemical composition of groundwater from alluvial aquifers in the Wanaka and Wakatipu basins, central Otago, New Zealand. *Hydrogeol J* 6:264–281
- Said R (1962) The geology of Egypt. Elsevier Pub. Co., Amsterdam, p 377
- Slimani R, Guendouz A, Trolard F, Moulla AS, Hamdi-Aissa B, Bourrie G (2015) Geochemical inverse modeling of chemical and isotopic data from groundwaters in Sahara (Ouargla basin, Algeria). *Hydrol Earth Syst Discuss.* <https://doi.org/10.5194/hess-2015-385>
- UNDP (2003) Fayoum human development report
- WHO (2004) Guidelines for drinking water quality, vol 1, 3rd edn (ISBN 92 4 1546387)
- WHO (2017) Guidelines for drinking water quality [electronic resource], 4th edn. Geneva, pp 307–441. http://whqlibdoc.who.int/publications/2011/97892_41548_151_eng.pdf (ISBN: 978 92 4 154815 1 (WEB version))
- Wolters W, Ghobrial NS, Bos MG (1987) Division of irrigation water in the Fayoum, Egypt. *Irrig Drain Syst* 1:159–172

Publisher's Note Springer Nature remains neutral with regard to jurisdictional claims in published maps and institutional affiliations.